4
Noise Removal Algorithms for the Heart Sound Signal

As discussed in Chapter 3, the noise components may contaminate the signal recording in real-life scenarios. The noise components may overlap the frequency band of Fundamental Heart Sound (FHS) and consequentially it may affect the diagnostic accuracy. Thus, there is a requirement of an efficient noise removal algorithm, which can suppress the in-band noise from the FHS. For this, a DWT based adaptive thresholding method for the heart sound signal is presented in this chapter. Moreover, in view of the importance of analysis of the heart sound signal in 'walking' scenario, an algorithm to remove noise components generated due to footsteps is also presented. The algorithm records heart sound signal and footstep signature using multiple axes accelerometer. The unwanted footstep signature present in the heart sound signal is removed judiciously. Thus, both the above-mentioned algorithms are proposed to be used sequentially to remove in-band noise as well as noise components generated due to footsteps.

In this chapter, first, the description of the DWT based denoising algorithm is provided and then the noise removal algorithm using multiple axes is discussed.

4.1 ADAPTIVE THRESHOLDING METHOD FOR WAVELET TRANSFORM BASED DENOISING OF THE HEART SOUND SIGNAL

In view of the requirement of an efficient denoising algorithm, a DWT based adaptive thresholding algorithm has been proposed and described as follows.

4.1.1 Introduction

Automatic analysis of the heart sound signal is generally performed in two steps; segmentation and classification [Jain and Tiwari, 2014; Moukadem et al., 2013]. In the segmentation step, FHSs are identified and then the signal is segmented into systole and diastole periods [Moukadem et al., 2013]. Systole is the time duration from S1 to S2 and the diastole is the time duration from S2 to next S1 [Jain and Tiwari, 2014]. In the classification step, the signal is classified as normal or abnormal having a particular disease. Thus, the primary task in the heart sound signal analysis is its segmentation [Moukadem et al., 2013]. However, the signal is highly susceptible to various noises generated due to the motion of subject, speech of subject, movement of the sensor, lung sounds, and ambient sources [Chourasia et al., 2014; Moukadem et al., 2013; Gradolewski and Redlarski, 2014]. Furthermore, pathologies may cause the presence of extra sound in the signal, called as murmur [Jain and Tiwari, 2014]. The presence of these components makes the segmentation task difficult. Therefore, to emphasise the S1 and S2, segmentation is often preceded by denoising to minimize the contamination level of noise and to remove the murmurs from the signal [Naseri et al., 2013; Patidar and Pachori, 2014]. However, the presence of murmurs in systole or diastole period and their time-frequency characteristics leads to a diagnosis of heart valvular diseases [Sanei et al., 2011; Dokur and Ölmez, 2008]. For example, murmur due to aortic stenosis, mitral regurgitation and pulmonary stenosis occur in systole period and aortic regurgitation and mitral stenosis occur in the diastolic period [Jain and Tiwari, 2014]. The features related to the murmurs can be extracted from the segmented cardiac cycles more efficiently as compared

to the signal with a number of cycles [Patidar and Pachori, 2014]. Therefore, once the signal is segmented into cardiac cycles, pathological features, if present, are extracted from these cycles [Patidar and Pachori, 2014].

Various denoising algorithms for the heart sound signal in time domain and frequency domain have been proposed [Leng et al., 2015]. In the time domain, denoising algorithms have been proposed based on conventional filters such as Chebyshev IIR filter [Bai and Lu, 2005], ANC, and autocorrelation method [Manikandan and Soman, 2010]. The conventional filters are limited to suppress the noise which is out of the frequency band of the signal components. On the other hand, ANC based algorithms such as LMS [Song et al., 2012; Tan et al., 2015], suppress the noise in an adaptive manner and, hence, suppress in-band noise as well. The major drawback of the ANC algorithms is that they need a reference (noise source) signal, which is not available in most cases of the real-life scenarios. Manikandan and Soman [Manikandan and Soman, 2010] proposed a computationally efficient denoising algorithm based on lag-1 autocorrelation method. However, the performance of these algorithms significantly degrades as the level of noise increases.

In the frequency domain based denoising algorithms, the time domain signal is first transformed into the frequency domain using a specific transform function such as Fourier transform and WT, and then the transformed signal is processed. Analysis of the sound signal in frequency domain provides the information about the spectral characteristics of the components presented in the signal and, hence, more efficiency in noise removal can be obtained as compared to the time domain. Sanei et. al. proposed an approach to separate the murmurs from the heart sound signal using singular spectrum analysis [Sanei et al., 2011]. Patidar and Pachori proposed an algorithm to remove murmurs using constrained tunable-Q wavelet transform [Patidar and Pachori, 2013]. However, both the algorithms require high computational time.

The most widely used method for the denoising of the heart sound signal is based on the DWT [Gradolewski and Redlarski, 2014; Vaisman et al., 2012; Debbal and Bereksi-Reguig, 2008b] due to the fact that the DWT coefficients of the heart sound signal components will be large and they will be confined to specific frequency band, while the coefficients for the noise components will have small amplitude and scattered in different frequency bands [Donoho and Johnstone, 1994]. Thus, denoising can be achieved by suppressing the small coefficients. However, the performance of the DWT based denoising algorithm significantly depends on the choice of the parameters: 1) Mother wavelet, 2) Number of decomposition levels and the levels to be processed, 3) Threshold value, and 4) Threshold function [Gradolewski and Redlarski, 2014].

For the denoising, mother wavelet should be orthogonal, which allows perfect reconstruction of the signal [Messer et al., 2001]. For the heart sound signal denoising, various orthogonal wavelets have been suggested such as Coiflet [Vaisman et al., 2012; Liu et al., 2012a], Symlet [Dokur and Ölmez, 2008] and Daubechies [Cherif et al., 2010; Naseri and Homaeinezhad, 2012]. In [Chourasia et al., 2014], Chourasia et. al. developed a new wavelet for the PCG signal of a foetus.

The second parameter is the number of decomposition levels. The number of decomposition levels should be selected precisely such that the useful signal components and unwanted components lie at different levels. The frequency range of each level depends on the sampling frequency of the signal. As the sampling frequency increases the frequency range of particular level increases [Meziani et al., 2012]. Therefore, different choices for a number of decomposition levels are reported in the literature [Messer et al., 2001; Gradolewski and Redlarski, 2014]. After the decomposition, levels to be processed should be chosen appropri-

ately. In literature, most of the algorithms processed all the decomposed levels [Messer et al., 2001; Gradolewski and Redlarski, 2014; Liu et al., 2012a; Agrawal et al., 2013], which requires unnecessary high computation. In other approaches, the signal is reconstructed using coefficients at a few selected levels, while discarding others [Cherif et al., 2010; Dokur and Ölmez, 2008; Naseri and Homaeinezhad, 2012]. These approaches removes only out-of-band noise. To suppress the in-band noise, the levels associated with the signal components should also be processed [Vaisman et al., 2012]. Researchers have also proposed algorithms for the appropriate selection of the levels based on the energy and the frequency range of the PCG signal [Safara et al., 2013; Choi, 2008].

The third parameter, threshold value, plays a crucial role in DWT based denoising. A large value of threshold affects the useful signal components, while a low threshold value will be ineffective to suppress the unwanted signal components [Naseri et al., 2013]. For the heart sound signal, mostly used threshold estimation methods are 'rigrsure' [Chourasia et al., 2014; Vaisman et al., 2012; Zhao, 2005], 'heursure' [Messer et al., 2001; Gradolewski and Redlarski, 2014], 'sqtwolog' [Agrawal et al., 2013], and 'minimaxi' [Gradolewski and Redlarski, 2014; Liu et al., 2012a]. The 'sqtwolog' is a fixed form method and does not take into account the content of the signal, but only depends on the length of the signal [Chourasia et al., 2014]. It provides a threshold value larger than other methods and hence it may result in over thresholding. 'minimaxi' is also a fixed form threshold method, in which the threshold value is estimated such that the maximum risk of estimation error is minimized [Messer et al., 2001]. The 'rigrsure' method determines a threshold value to minimize the Stein's Unbiased Risk Estimation (SURE). 'rigrsure' and 'minimaxi' methods estimate threshold value to minimize the risk estimation and results in the low threshold value [Cai and de B. Harrington, 1998]. The 'heursure' method selects one of the methods from the 'sqtwolog' and 'rigrsure' methods, based on the comparison between the SURE estimation and SNR [Messer et al., 2001]. Naseri and Homaeinezhad [Naseri and Homaeinezhad, 2012] devised a threshold estimation method based on the weighted variance of the noise while Kumar and Saha [Kumar and Saha, 2014] calculated the threshold as the 20% of the weighted maximum energy of the coefficient vector. However, values of parameters used in these methods were obtained heuristically.

The fourth parameter is the threshold function, which defines the way to treat the wavelet coefficients using the estimated threshold value. Soft and hard are two existing threshold functions used extensively for the denoising of heart sound signals [Chourasia et al., 2014; Vaisman et al., 2012; Liu et al., 2012a]. In soft threshold function, the coefficients lower than the threshold are replaced by zeros while other coefficients get shrank by the threshold value [Chourasia et al., 2014]. In hard threshold function, the coefficients lower than the threshold are replaced by zeros, as in soft threshold, while larger coefficients remain unchanged. Hard threshold function may cause discontinuities in the reconstructed signal and make it oscillating [Messer et al., 2001]. In soft threshold function, shrinkage of the wavelet coefficients by threshold reduces the effect of singularities and transients that cannot be addressed by the hard threshold function [Luo and Zhang, 2012]. However, hard threshold function produces a larger SNR value than the soft threshold function. Zhao [Zhao, 2005] proposed a generalized threshold function although it needs a selection of parameter, which controls the performance of the algorithm.

To address the issues discussed above related to threshold estimation and threshold function, we propose a new DWT based denoising algorithm for the heart sound signals. We used 'Coif-5' wavelet as a mother wavelet and performed five levels of decomposition of the signal sampled at 2 kHz. When a signal with 2 kHz sampling frequency is decomposed, the 4^{th} and 5^{th} levels cover the frequency range 31-125 Hz, approximately [Singh and Anand, 2007], and hence cover most of the frequency range of the S1 and S2, which is 25-120 Hz [Singh and Anand, 2007]. Therefore, in the proposed algorithm, only these two levels are processed.

Removal of the coefficients of lower detailed levels also removes the out-of-band noise. To further improve the performance of the denoising, we propose a novel adaptive threshold estimation method using statistical properties of the DWT coefficients. The proposed method uses the domain knowledge that the sum of the length of the S1 and S2 remains less than 25% of the length of a cardiac cycle [Naseri and Homaeinezhad, 2013; Atbi et al., 2013]. Therefore, a new parameter, med_{75} is calculated instead of traditional median value. The med_{75} represents the 75^{th} percentile value in the sorted absolute values of a coefficient vector in ascending order. Further, to address the issue of threshold function, we also propose a new method called as 'non-linear mid' function for the heart sound signal. Furthermore, its parameters are optimized using the genetic algorithm, to improve its performance for the heart sound signals. Thus, the proposed algorithm adaptively shrinks the wavelet coefficients of the signal.

4.1.2 Methodology

The proposed algorithm calculates a threshold value adaptively and the same is applied to the wavelet coefficients of selected levels. The proposed algorithm performs in three steps as described below.

(a) Decomposition of the Signal

The first step in DWT based denoising is the decomposition of the signal into approximation (A) and detailed (D) coefficients. These coefficients can be obtained by applying analysis filters: low pass filter (H) and high pass filter (G). To obtain the coefficients at the next level, the output of the lowpass filter, called as approximation coefficients, and output of highpass filter, called as detailed coefficients, are decimated by a factor of two and then both the analysis filters are applied to the decimated approximation coefficients. These two steps are applied recursively to obtain coefficients at higher levels, as shown in Figure 4.1. This decomposition algorithm is called as Mallat algorithm and the constructed tree is called as Mallat decomposition tree [Mallat, 1989].

In the proposed algorithm, 'Coif-5' wavelet is chosen as the mother wavelet because it gives better performance for the denoising of heart sound signal as compared to other wavelets [Gradolewski and Redlarski, 2014; Messer et al., 2001; Liu et al., 2012a]. Using the 'coif-5' wavelet, the signal is decomposed up to five levels. Decomposition of the signal with 2 kHz sampling frequency will result in five detailed levels (500-1000, 250-500, 125-250, 62-125, and 31-62 Hz) and one approximation level (0-31 Hz) [Singh and Anand, 2007]. Thus, the 4^{th} and 5^{th} detailed levels cover most of the frequency range of FHS, which is typically 25-120 Hz [Singh and Anand, 2007] and hence FHS are prominently present in these two levels, as shown in Figure 4.2. Therefore, only these two levels are processed further while other detailed level coefficients and approximation coefficients are discarded. Non-inclusion of lower level detailed coefficients also suppress the murmurs from the signal because fre-

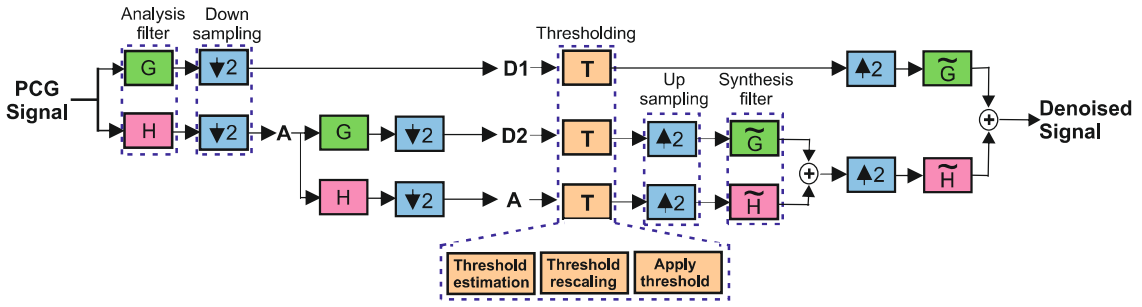

Figure 4.1 : Block diagram of the DWT based denoising algorithm

quency range of most of the murmurs is higher than the frequency range of S1 and S2 [Debbal and Bereksi-Reguig, 2008a]. The suppression of the murmurs is required to emphasise the S1 and S2. However, the characteristic features of the murmur are needed for the diagnosis of the heart valve diseases. Hence, these features will be required and the same can be extracted after the signal is segmented into cardiac cycles.

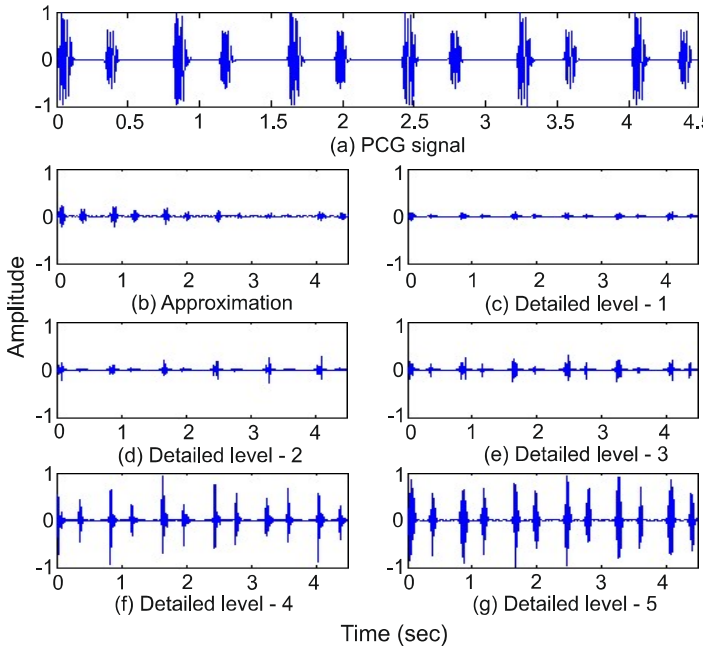

Figure 4.2 : Reconstructed signal at various detailed levels and approximation level

(b) Thresholding of the Coefficients

The second step is thresholding of the wavelet coefficients, in which the coefficients are modified based on a threshold value. Generally, thresholding of the coefficients is performed in three steps [Gradolewski and Redlarski, 2014], described in following subsections.

Estimation of the threshold

As stated in the introduction section, the existing methods are either not adaptive to the SNR of the signal or try to minimize the risk for the worst case. The threshold value should be a function of the SNR of the signal so that the noise can be suppressed efficiently without, or minimally, affecting the useful signal components. In view of this requirement, a novel method of threshold estimation based on characteristics of the signal is proposed and given as follows.

In this method, a new parameter is obtained to estimate the noise level based on the time domain information of the heart sound signal. A detailed time-domain analysis of multiple heart sound signals is provided in [Singh and Anand, 2007]. According to it, the sum of time duration of S1 and S2 remains less than 25% of the time duration of a cardiac cycle. Same observations are also reported in [Naseri and Homaeinezhad, 2013; Atbi et al., 2013] for normal and various pathological cases. Thus, 75^{th} percentile value of the absolute values of the signal, sorted in ascending order, indicates the level of noise present in the signal, as shown in Figure 4.3(a). Furthermore, the 75^{th} percentile value gives effective indication of the noise level as compared to the 50^{th} percentile value (median), as shown in Figure 4.3(b). Therefore, we propose a new variable med_{75}, which represents 75^{th} percentile value of the sorted absolute values of coefficient vector in ascending order, and used for the estimation of the threshold value.

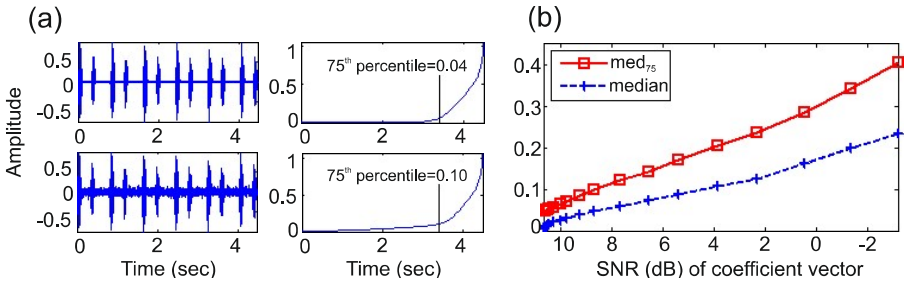

Figure 4.3 : Statistical parameters for the signal with added white Gaussian noise: (a) med_{75} at two different SNR values and (b) med_{75} and median values at various SNR values

Figure 4.4 provides the analysis of the med_{75} parameter and statistical parameters, mean ($m = mean(|D_j|)$) and variance ($v = variance(|D_j|)$), of the absolute of the coefficient vector (D_j) contaminated with noise at three different levels, low, moderate, and high. As shown in the figure, in the first case, when the med_{75} is lower than the variance (v) and mean (m), the noise level is very low and therefore the threshold value should be low. In this case, the difference between the med_{75} and variance (v) is proportional to SNR of the signal, as shown in Figure 4.5. The second case, when the med_{75} is larger than the variance (v) and smaller than the mean (m), represents a signal contaminated with a moderate level of noise. In the third case, where noise level is very high, the med_{75} is larger than the mean (m) and variance (v) both. Therefore, the threshold value should be high. In this case, as shown in Figure 4.5, difference between the med_{75} and mean (m) increases with decrease in SNR. Based on these observations of the relationship between three parameters, mean (m), med_{75}, and variance (v), the threshold estimation is proposed as follows:

$$T = \begin{cases} med_{75} \times [1 - (v - med_{75})] & if(med_{75} < v) \quad Case: 1 \\ med_{75} & if((med_{75} > v) \;\&\&\; (med_{75} < m)) \quad Case: 2 \\ med_{75} + (med_{75} - m) & if(med_{75} > m) \quad Case: 3 \end{cases} \tag{4.1}$$

In the first case, the threshold is obtained by multiplying med_{75} and $(1 - (v - med_{75}))$, as given in Eq.(4.1), to obtain a small value of threshold. In this case, the multiplying factor $(1 - (v - med_{75}))$ will increase with the decrease in SNR and consequentially the threshold value will increase. As the value of med_{75} reaches close to the variance (v), the multiplying factor tends to be one and hence threshold becomes close to med_{75} value. In the second case, the threshold value is set equal to the med_{75}. As the level of noise increases further, the med_{75} will also increase (shown in Figure 4.5) and consequentially the threshold value will increase. In the third case where threshold value should be high, difference between the med_{75} and mean (m) increases with decrease in SNR, as discussed above. Therefore, the threshold is obtained by summing the med_{75} and the difference of the med_{75} and mean (m), as given in Eq.(4.1).

Threshold Rescaling

After the estimation of the threshold value, it is rescaled according to the level of noise present in the signal. The Multiple-scale dependent (mln) [Misiti et al., 1996] rescaling approach is used to rescale the estimated threshold value T. According to it, the variance of the noise is estimated for each level and the threshold value is rescaled i.e multiplied by the variance of the noise. Since the noise variance (σ) is unknown in most cases, it is estimated as

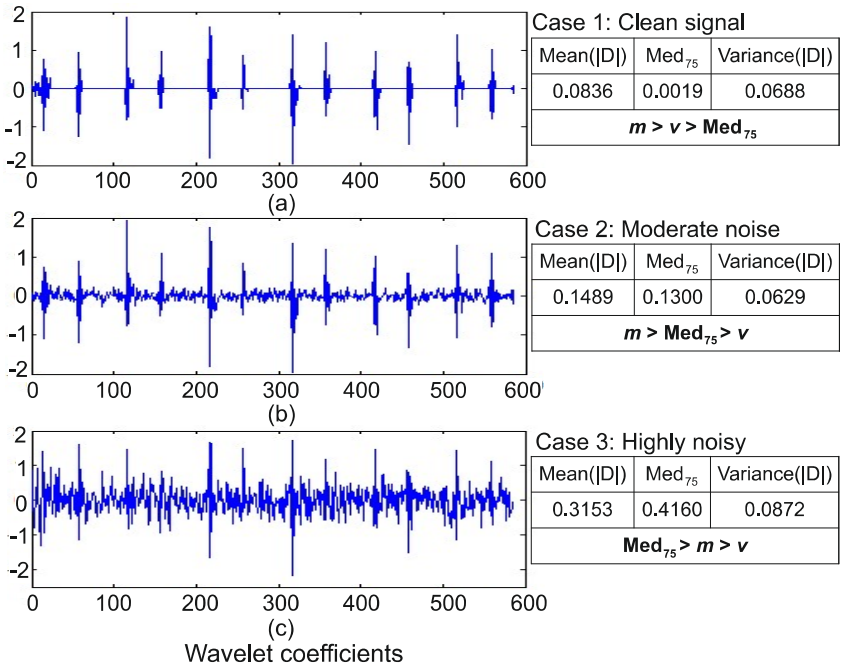

Figure 4.4 : Statistical parameter analysis for the wavelet coefficients (detailed level-4) in three different cases (a) Low level of noise, (b) Moderate level of noise, and (c) Highly noisy

follows [Chourasia et al., 2014]:

$$\widehat{\sigma} = \frac{MAD\{D_j[n]\}}{0.6745} \tag{4.2}$$

where $MAD\{D_j\}$ represents the median of absolute value of detail coefficients at level j.

Applying Threshold to the Coefficients

The third step is to apply the scaled threshold value to the wavelet coefficients using a threshold function. Mostly used threshold functions for the heart sound signal are 'soft' and 'hard' functions [Luo and Zhang, 2012]. As discussed in Section 1, the hard function produces a larger SNR value than the soft function. However, the hard function may cause discontinuities in the denoised signal. To overcome these shortcomings, another threshold function, called as *mid* function [Phinyomark et al., 2012] is explored to use for the heart sound

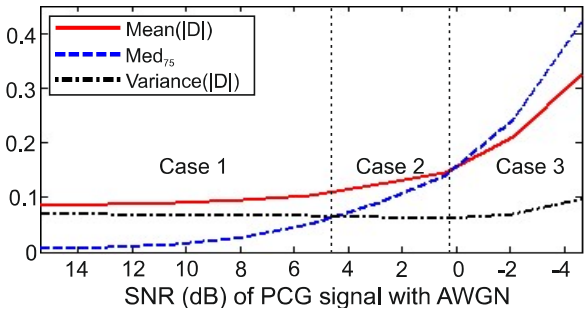

Figure 4.5 : Statistical parameters (mean, Med_{75}, and variance) of the wavelet coefficients (detailed level-4) of signal contaminated with white Gaussian noise at various levels

signals. As shown in Figure 4.6, it uses two threshold values, T_1 and T_2, given as follows:

$$T_1 = \alpha \times T \tag{4.3}$$

$$T_2 = \beta \times T \tag{4.4}$$

The wavelet coefficients are treated in three partitions: 1) retain the coefficients with large values unchanged, 2) coefficients with small values are set to zero, and 3) linearly shrink moderate value coefficients by the threshold, as follow.

$$D_{j\ mid}^{T}[k] = \begin{cases} D_j[k] & if|D_j[k]| > T_2 \\ sign(D_j[k])(|D_j[k]| - T_1) & if T_1 \leq |D_j[k]| \leq T_2 \\ 0 & if|D_j[k]| < T_1 \end{cases} \tag{4.5}$$

Thus, this threshold function overcomes the issue of soft threshold function by retaining large coefficients without change, while reduces the issue of discontinuities by linearly shrinking of the middle coefficients. However, the mid function also contains discontinuities as in case of soft and hard functions. To resolve this issue of the 'mid' function, the linear behaviour of the function in the range of T1 to T2 is transformed into the non-linear behaviour to form a 'non-linear mid' function as follows:

$$D_{j\ non-linear\ mid}^{T}[k] = \begin{cases} D_j[k] & if|D_j[k]| > T_2 \\ D_j[k]^3/T_2^2) & if T_1 \leq |D_j[k]| \leq T_2 \\ 0 & if|D_j[k]| < T_1 \end{cases} \tag{4.6}$$

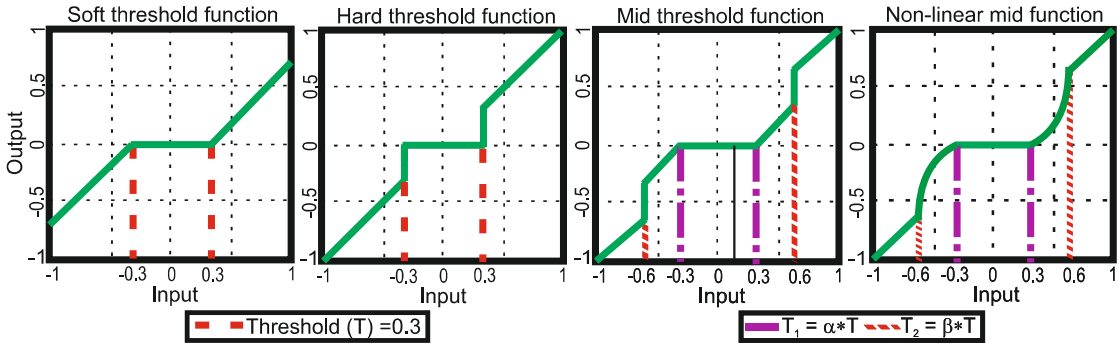

Figure 4.6 : Output response of the soft, hard and mid threshold functions.

Optimisation of parameters α and β

In [Phinyomark et al., 2012], value of α was set to one and value of β was set to two. In this work, the values of α and β parameters are optimised to improve the performance of the 'non-linear mid' threshold function for the heart sound signal. For the optimization, the genetic algorithm (GA) is used because it is found to be more effective in global optimization [Yuan et al., 2010]. The GA is an adaptive heuristic search algorithm based on the evolutionary ideas of natural selection in which stronger individuals are likely be the winners in a competing environment [Man et al., 1996]. The algorithm repeatedly modifies a population of individual solutions and, over successive generations, the population evolves toward an optimal solution [Man et al., 1996]. The algorithm is implemented with the help of MATLAB® (MathWorks) global optimization toolbox. The objective function is to minimize the mean square error (*MSE*) between the coefficients of clean signal and the thresholded coefficients, as follows:

$$MSE = \frac{1}{N}\sum_{n=1}^{N}\left[D_j^{clean}(n) - D_j^{T}(n)\right]^2 \tag{4.7}$$

where N is the length of vector, D_j^{clean} is a coefficient vector of j^{th} level of the clean signal, and D_j^T is thresholded coefficient vector of j^{th} level of the noise contaminated signal. Based on the obtained results of optimisation by the Genetic algorithm, the value of α is found to be one for all noise levels. This was an expected value as the coefficients having an amplitude smaller than the threshold value (T) should be zero and this will happen with $\alpha = 1$, as this can be seen from Eq.4.8. On the other hand, the value of β is obtained to be a function of noise level. This is given as follows:

$$\beta = \begin{cases} 1.3 & med_{75} \leq v \\ 1.4 & med_{75} > v \end{cases} \tag{4.8}$$

In case of low noise ($med_{75} \leq v$), the value of β should be low. We expected the value of β to be large for the high noise case. However, since the value of estimated threshold (T) itself is large, the optimum value of the second threshold $(T_2 = \beta \times T)$ is obtained at a moderate value of β (in this case 1.4), as against 2 given in [Phinyomark et al., 2012].

(c) Reconstruction of the Signal

After thresholding of the coefficients, the signal is reconstructed from the thresholded coefficients. To reconstruct, the highest level detailed and approximation coefficients are up-sampled by two and passed through the high pass filter ($\widetilde{G}$) and low pass filter ($\widetilde{H}$), respectively [Mallat, 1989]. The summation of the outputs of these two filters results in approximation coefficients for the next level reconstruction, as shown in Figure 4.1. $\widetilde{G}$ and $\widetilde{H}$ are called as synthesis filters and they are orthogonal to the analysis filters. The synthesis filters have relation with the analysis filters such that all four filters, two analysis filters and two synthesis filters, form quadrature mirror filters [Chourasia et al., 2014].

In the proposed method, detailed coefficients at level 4^{th} and 5^{th} are thresholded according to the proposed thresholding method, as discussed previously. The coefficients at detailed levels 1^{st}, 2^{nd}, and 3^{rd} and the approximation coefficients are made zero. Thus, the reconstructed signal contains the signal corresponding to the thresholded coefficients at 4^{th} and 5^{th} levels.

4.1.3 Results and Discussion

The Experiments are performed on the heart sound signal contaminated with simulated white Gaussian noise. For the noise simulation, pink and red noise models are also considered because Gradolewski and Redlarski [Gradolewski and Redlarski, 2014] observed that the characteristics of real-life noise are similar to pink and red noises. Furthermore, the performance of the proposed method is also analysed on the signal acquired in real-life scenarios. To show the efficacy of the method to remove the murmur sounds, it is applied to various pathological signals obtained from publicly available database [eGeneralMedical].

Performance evaluation indices: For the quantitative evaluation of the methods, following three parameters are used.

A) Signal-to-noise ratio (SNR): SNR is most commonly used parameter to evaluate the performance of denoising algorithms. The expression for SNR is given as follows [Gradolewski and Redlarski, 2014].

$$SNR_{dB} = 10 \times \log_{10}\left(\frac{Signal\ power}{Noise\ power}\right) \tag{4.9}$$

B) Fit coefficient: Fit coefficient, proposed in [Gradolewski and Redlarski, 2014] for the performance evaluation of denoising algorithm for the heart sound signals, shows if the in-

formation about subject's health is preserved. It is obtained as follows.

$$fit = 100 \times \left(1 - \frac{\sum_{i=1}^{N}[f_2(i) - f_1(i)]^2}{\sum_{i=1}^{N}\left[f_1(i) - (1/N)\sum_{j=1}^{N} f_1(j)\right]^2}\right) \tag{4.10}$$

where f_1 is clean signal and f_2 is the denoised signal. This coefficient indicates the difference in morphology of the denoised signal f_2 with respect to the clean signal f_1. Basically, it is a normalized coefficient of determination in the range of 0% to 100% [Everitt and Skrondal, 2010]. It is used in the statistical model analysis to assess goodness of fit of a model. The value of fit will be 0% when signals are mismatched and the information is lost, and 100% when there is a perfect match between the signals.

C) Detection rate of S1 and S2: To show the diagnostic significance of the method, the detection rate of the FHS, S1 and S2, are obtained. The detection rate shows the percentage of correctly detected components in the denoised signal using a particular method. Detection of components is achieved by a threshold-based peak finding algorithm presented in [Liang et al., 1997]. Figure 4.7 shows the PCG signal, its envelope extracted using normalized average Shannon energy, and the components detected by the algorithm [Liang et al., 1997].

A number of false detected components are also obtained. A small number of false components with high detection rates of S1 and S2 show that the method is efficient to suppress the noise. If the number of false components is low and detection rate of the components is also low, it means the threshold value is high and thus resulted in over thresholding. On the other hand, a large number of false points shows the inefficacy of the threshold method to suppress the noise.

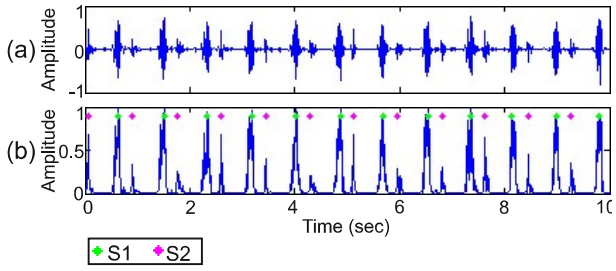

Figure 4.7 : Peak detection and identification: (a) PCG signal, and (c) envelope of the signal with identified components

Database used for experiments: The experimental results are obtained using two datasets of PCG signals. First is taken from the eGeneralMedical [eGeneralMedical], which includes PCG signal for normal and various pathological cases. This dataset does not include the PCG signals contaminated with real-life noise. Therefore, a second dataset is created by acquiring PCG signals from ten subjects in clinical and noisy environments, each for 20 seconds duration. For both the datasets, the sampling frequency is set to 2 kHz. The sampling rate of 2 kHz is sufficient for the PCG signal because its fundamental components and pathological sounds, murmurs, lie below 800 Hz frequency [Moukadem et al., 2013; Gradolewski and Redlarski, 2014].

The proposed threshold estimation method uses med_{75}, as discussed in the previous section, to measure the level of noise in the signal. To be effective of med_{75}, the signal under consideration should cover at least one cardiac cycle. Therefore, in the proposed method, the signal is segmented into non-overlapping windows and the length of the window is set to 2 seconds. This length will cover the one cardiac cycle until the heart rate does not go less than 30 beats per minute.

State-of-the-art methods: Performance of the proposed method is compared with the performance of DWT based denoising methods reported in literature [Messer et al., 2001; Gradolewski and Redlarski, 2014; Liu et al., 2012a]. Messer et. al. [Messer et al., 2001], and Gradolewski and Redlarski [Gradolewski and Redlarski, 2014] performed experiments to determine the optimum parameters of DWT for denoising of the PCG signals. Based on the experimentally determined optimum parameters, for the comparison, we used 'Coif-5' as mother wavelet, 'mln' as rescaling method and following two combinations of threshold estimation methods and threshold function.

DWT-A: 'rigrsure' threshold with soft threshold function.

DWT-B: 'minimaxi' threshold with hard threshold function.

Approximation coefficients were discarded because they are out-of-frequency band of FHS, as observed in Figure 4.2.

(a) Results for the PCG Signal with Added White Gaussian Noise

Although white Gaussian noise characteristics were not observed in real-life noise [Gradolewski and Redlarski, 2014], the proposed method is applied to the PCG signal with Additive White Gaussian Noise (AWGN) to analyse its efficacy to suppress it. Experiments were performed on the PCG signals acquired from 10 subjects. These signals were acquired in a clinical scenario and then multiple instances of white Gaussian noise were added at various input SNR. The obtained qualitative results using various methods, at -4.63 dB SNR, are shown in Figure 4.8. This SNR value is obtained when the white Gaussian noise is added with 10 dB SNR per sample to the signal using MATLAB® (MathWorks). The obtained quantitative results are provided in terms of SNR and fit values in Table 4.1 as mean$\pm$standard deviation and in terms of detection rates in Figure 4.9, for all subjects at various levels of SNR.

Results of the proposed threshold estimation method with threshold functions including soft, hard, mid and proposed mid are analysed and compared with all four threshold estimation methods ('sqtwolog', 'rigrsure', 'heursure', and 'minimaxi'), separately.

Soft threshold function: The proposed threshold estimation method and all the four methods with soft threshold function are applied to the PCG signal with AWGN. From Figure 4.8(a)-(e), it can be observed that the proposed threshold estimation method is outperforming all popular methods. 'rigrsure' and 'heursure' are also providing satisfactory results with soft threshold function, while 'sqtwolog' method results into over thresholding.

From the Table 4.1, it can be observed that the SNR values are higher of the denoised signal using the proposed threshold estimation method compared to other methods. The same result can also be observed for the fit coefficient. At a low level of noise (SNR $>$ 0.38 dB), 'heursure' method is giving similar performances as that of the proposed method. On the other hand, at a high level of noise (SNR $<$ 0.38 dB), 'rigrsure' method is producing higher SNR and fit values than the 'heursure' method.

Hard threshold function: Similarly, experiments are performed with the hard threshold function. From the Figure 4.8(a)-(e), it can be observed that the proposed threshold estimation method outperforms competitive methods. However, the denoised signal has discontinuities, which is expected in the case of the hard threshold function. Figure 4.8(a), in particular, shows that 'sqtwolog' suppressed the noise significantly. However, it results in over thresholding and consequentially, PCG signal's useful components also got suppressed.

As shown in Table 4.1, at a high level of noise (SNR $<$ 5.42 dB) the proposed method is producing highest SNR values when compared to state-of-the-art methods. However, at low levels of noise (up to 5.42 dB), 'sqtwolog' method is producing highest SNR values among all

methods. But, 'sqtwolog' may suppress the heart sound components and it may lead to wrong diagnosis [Gradolewski and Redlarski, 2014]. Higher fit values for the proposed threshold estimation method also demonstrate the superiority of it over the compared methods. In the comparison of soft and hard threshold functions, the hard function produces higher SNR and fit values than the soft function. However, the result of the hard function contains few noise components. These results are in line with the reported works in literature [Luo and Zhang, 2012].

Mid and proposed non-linear mid threshold functions: The results are obtained using the proposed threshold estimation method with mid and proposed mid threshold functions separately, and plotted in Figure 4.8(f). From the figure, it can be observed that the threshold value obtained by the proposed threshold estimation method with the mid function suppresses the noise effectively. The quantitative effectiveness of the proposed threshold estimation method in terms of SNR and Fit values can be found in Table 1. From the table, it can be observed that the proposed threshold estimation method with mid function produces higher SNR and fit values when compared to the values obtained using the soft and hard functions. These observations show that the mid function overcomes the issues related to both soft and hard threshold functions. The proposed threshold estimation method also ensures that there is no significant loss in PCG signal components and hence diagnostic information present in the signal are preserved. However, there is some loss of information due to the use of the mid function [Phinyomark et al., 2012], as can be seen in Figure 4.8(f) at time instant 2.7 sec, S2 component is suppressed. This loss of S2 is because the value of β (two as in [Phinyomark et al., 2012]) is high and consequentially the upper limit (T_2) of coefficient shrinking is also high. This issue is addressed in the proposed non-linear mid threshold function by tuning the parameter β, hence the results are improved as shown in Figure 4.8(f), second column.

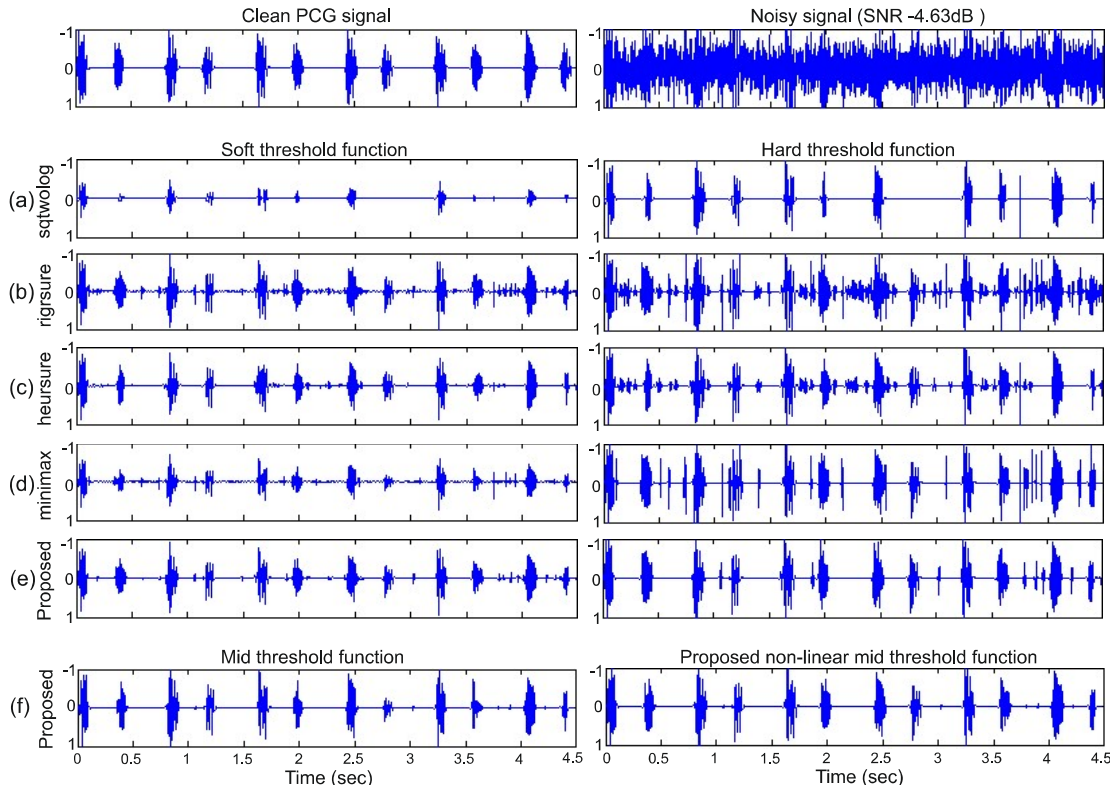

Figure 4.8 : Denoising results for soft, hard, mid, and non-linear mid threshold functions with various thresholds estimated by different methods: (a) 'sqtwolog', (b) 'rigrsure', (c) 'heursure', (d) 'minimaxi', (e) and (f) proposed threshold estimation method

The figure depicts that the proposed method (proposed threshold estimation method with proposed mid function) is able to suppress the noise from the PCG signal with AWGN at low SNR -4.63 dB. The SNR and fit values obtained using the proposed method given in Table 4.1, are highest among all the methods. There is a significant improvement in SNR and fit values for the proposed method at a higher level of noise.

Table 4.1 : Obtained SNR (in dB) of the denoised PCG signals (average of 10 instances ± standard deviation) contaminated with simulated white Gaussian noise

	SNR after denoising (dB)				Fit coefficient (%)			
SNR due to addition of AWGN	10.38±0.04	5.42±0.05	0.38±0.04	-4.63±0.04	10.38±0.04	5.42±0.05	0.38±0.04	-4.63±0.04
Soft threshold function								
sqtwolog	12.74±0.16	8.30±0.25	3.97±0.20	0.76±0.11	99.76±0.02	97.96±0.09	84.83±0.13	31.56±0.26
rigrsure	16.35±0.27	11.91±0.17	7.26±0.25	2.78±0.43	99.96±0.01	99.75±0.03	97.73±0.04	78.55±0.31
heursure	16.44±0.26	12.08±0.26	7.53±0.20	2.59±0.23	99.97±0.01	99.76±0.01	97.49±0.03	73.30±0.26
minimaxi	14.41±0.17	10.02±0.27	5.61±0.21	1.85±0.14	99.89±0.01	99.11±0.01	92.94±0.05	60.17±0.25
proposed	16.54±0.24	12.18±0.26	7.59±0.18	3.07±0.21	99.97±0.01	99.75±0.01	97.66±0.06	82.59±0.23
Hard threshold function								
sqtwolog	19.13±0.18	14.80±0.26	8.11±0.33	2.33±0.35	99.98±0.00	99.88±0.01	97.37±0.02	62.11±0.41
rigrsure	14.79±0.45	9.84±0.46	4.99±0.43	1.14±0.75	99.95±0.01	99.51±0.03	95.19±0.15	54.65±0.21
heursure	15.34±0.46	10.61±0.28	5.99±0.55	1.95±0.50	99.96±0.01	99.69±0.02	96.86±0.10	65.18±0.19
minimaxi	17.72±0.32	13.09±0.25	7.96±0.40	2.48±0.40	99.97±0.01	99.74±0.07	97.15±0.18	67.13±0.22
proposed	18.54±0.37	14.47±0.37	8.86±0.43	3.43±0.25	99.98±0.01	99.88±0.01	98.14±0.03	82.77±0.13
Mid threshold function								
proposed	19.05±0.19	14.86±0.21	8.98±0.18	3.52±0.27	99.98±0.01	99.89±0.01	98.32±0.08	83.09±0.24
Proposed non-linear mid threshold function								
proposed	19.18±0.21	14.89±0.25	9.51±0.37	4.03±0.15	99.98±0.01	99.89±0.02	98.61±0.09	85.09±0.21

Same results are also observed for the detection rate of S1 and S2 using the proposed method, as shown in Figure 4.9 (a and b). The detected number of false points is also lowest among all methods. These results show the diagnostic superiority of the proposed method over state-of-the-art methods.

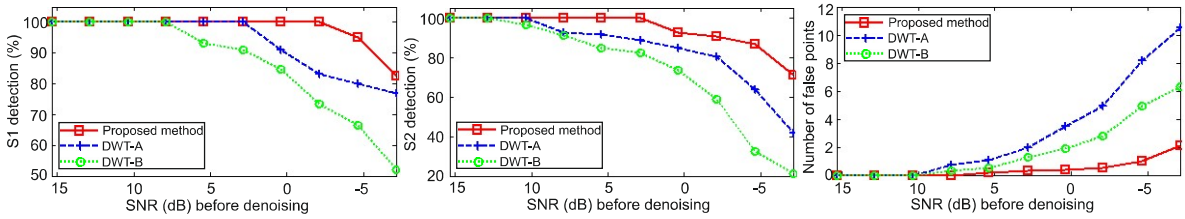

Figure 4.9 : Results for PCG signals of different subjects with AWGN: (a) Detection rate of S1, (b) Detection rate of S2, and (c) Number of false points

(b) Results in Case of Pink and Red Noise

The proposed method is also applied to the PCG signals contaminated by simulated pink noise and red noise, generated through MATLAB® code created by Hristo Zhivomirov [Zhivomirov]. The obtained denoised signals are given in Figure 4.10. The figure shows the superiority of the proposed method over state-of-art methods. To quantify the results, in addition to the waveforms given in Figure 4.10, we obtained SNR and fit values of the denoised signal at various noise levels as shown in Figure 4.11. The figure elucidates that the proposed method significantly improves the SNR values of the denoised signal and produces higher fit values. Furthermore, as in the case of AWGN, our methods give higher detection rates of S1 and S2, as shown in Figure 4.12, and at the same time, gives a lower number of false points. It shows that the proposed method is efficient to suppress the pink and red noises, which have similar characteristics to real-life noise.

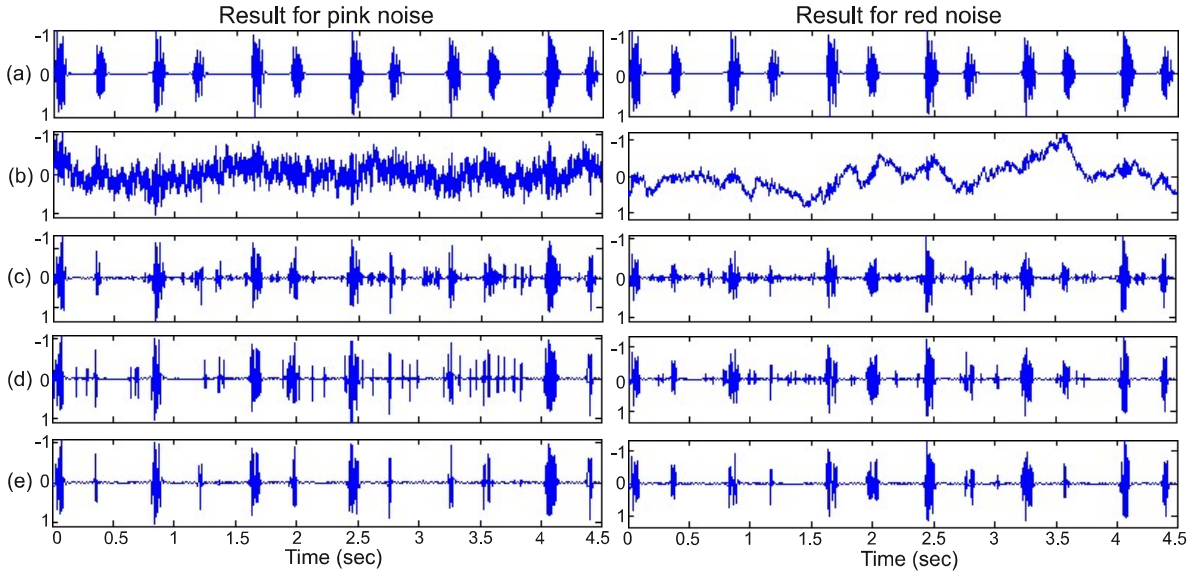

Figure 4.10 : Obtained denoising results for the PCG signal contaminated with pink and red noise: (a) Clean signal, (b) Noisy signal, (c) DWT-A, (d) DWT-B, and (e) Proposed method

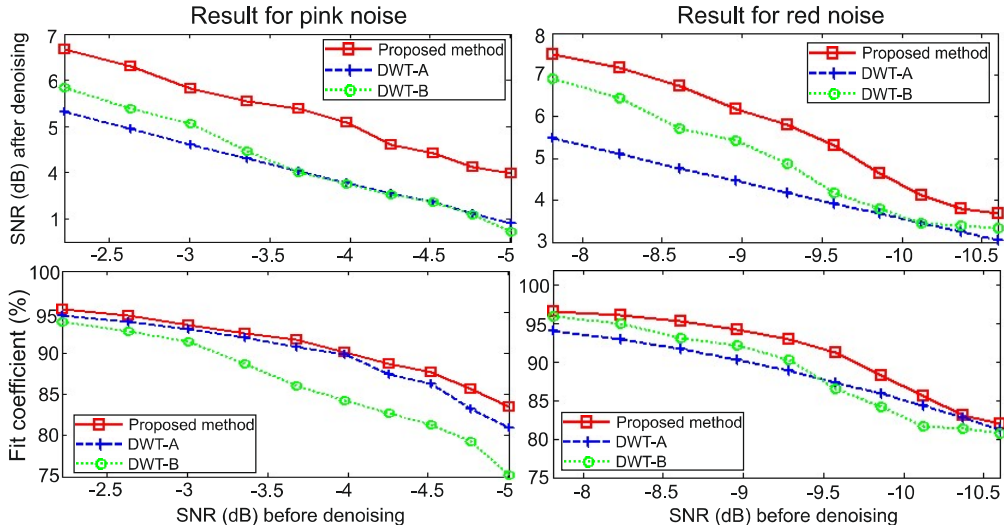

Figure 4.11 : SNR and fit values for the denoised PCG signal contaminated with pink and red noise

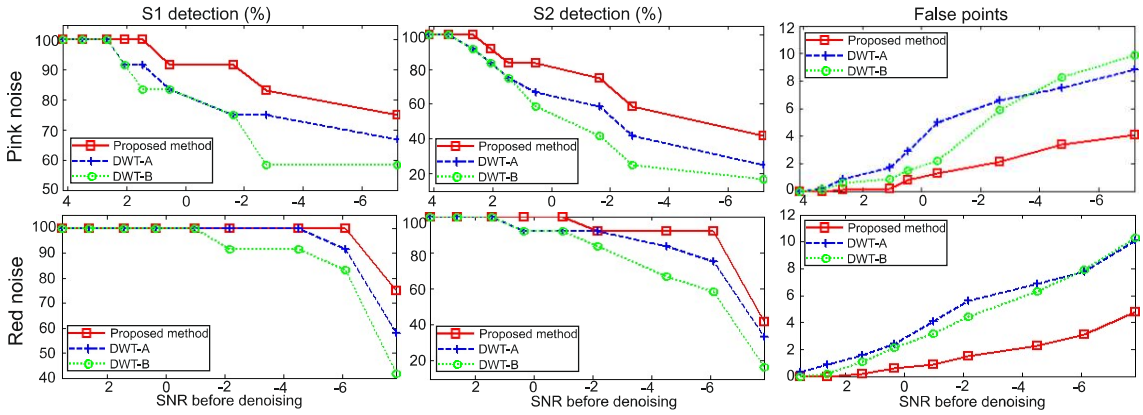

Figure 4.12 : Detection rate of S1 and S2 and number of false points in the denoised PCG signal contaminated with pink and red noise.

(c) Results for the PCG Signal Recorded in Real-life Scenarios

As discussed in Section 4.1, the heart sound signal is vulnerable to various noises generated in real-life scenarios. Therefore, it is of paramount importance to analyse the efficacy of the proposed method under such scenarios. For this purpose, signals are recorded from different subjects when they were moving and speaking, while working in an office where there were other sources of noise such as noise due to another person talking. Figure 4.13 shows qualitative, and Table 4.2 gives a quantitative performance evaluation of the results of the proposed method as compared to the state-of-art methods. The figure shows the performance superiority of the proposed method over the compared methods. The detection rate of S1 and S2, and number of false points are presented in Table 4.2. The numbers quantify the efficacy of the proposed method over state-of-the-art methods.

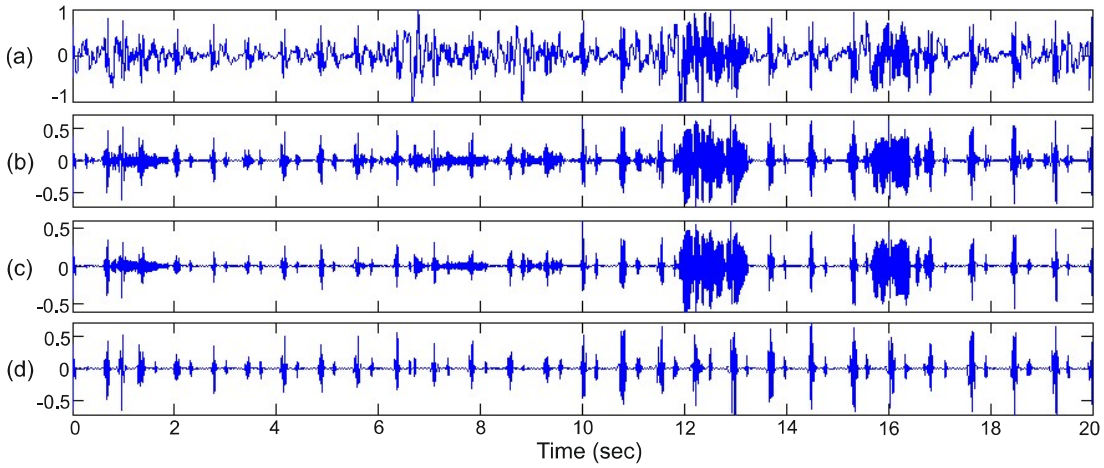

Figure 4.13 : Denoising results for the recorded PCG signal in noise scenario using various methods: (b) DWT-A, (c) DWT-B, and (d) Proposed method

Table 4.2 : Result for the PCG signals contaminated with noise generated in real-life scenarios

S. No.	Heart rate	% of S1 detection			% of S2 detection			False points		
		DWT-A	DWT-B	Proposed	DWT-A	DWT-B	Proposed	DWT-A	DWT-B	Proposed
1	68	100	100	100	100	90.9	100	1	0	0
2	69	90.9	90.9	100	81.8	72.7	90.9	4	6	1
3	71	100	100	100	91.6	100	100	2	0	0
4	74	91.6	91.6	100	75	83.3	91.6	4	4	2
5	74	100	100	100	91.6	83.3	100	1	4	1
6	76	92.3	92.3	100	76.9	84.6	92.3	4	3	0
7	78	100	100	100	92.3	84.6	100	3	5	1
8	81	100	100	100	100	92.8	100	0	1	0
9	84	93.3	93.3	100	80	73.3	100	4	7	0
10	88	93.3	93.3	93.3	66.6	73.3	86.6	7	5	2

As discussed in the previous chapter, in 'walking' scenario, noise generated due to footsteps contaminate the heart sound signal. It is also discussed that the patients with CVDs or who are prone to CVDs should walk for at least 30 minutes daily. Thus, a system which can perform effectively in 'walking' scenario would be very helpful. Therefore, the proposed method is tested especially on the signal acquired when the subject was walking. Figure 4.14 shows the results obtained using various methods. From the figure, it can be observed that the proposed method suppressed the noise components significantly as compared to other methods. However, the noise components generated due to footsteps are presented (at time instance (second) 3.2, 5.6, 7.2, 8.1, 9.3, 10.2, 11.6, 12.5, 16.4, 17.5, 18.5, 19.6) in the denoised signal sing the proposed method.

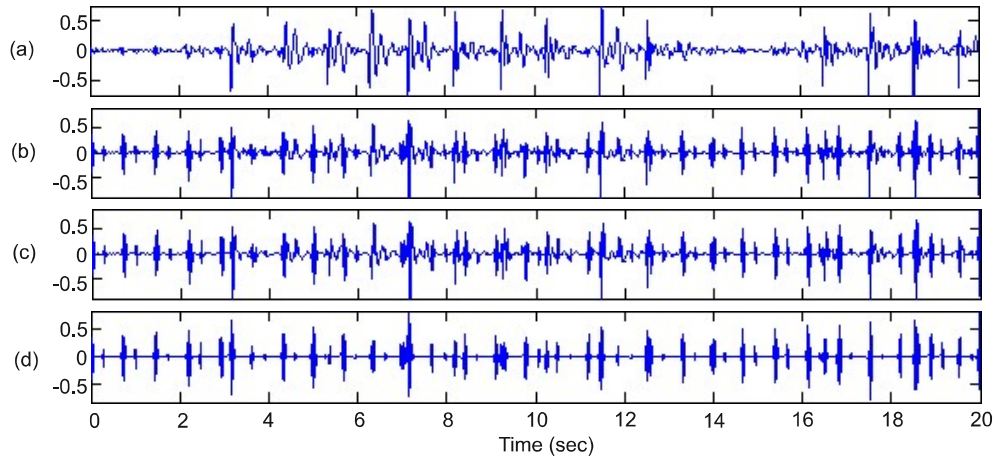

Figure 4.14 : Denoising results for the recorded PCG signal in 'walking' scenario using various methods: (b) DWT-A, (c) DWT-B, and (d) Proposed method

(d) Results for PCG Signal with Murmur Sound

In order to evaluate the efficacy of the proposed method's ability to emphasise the S1 and S2 in the presence of murmurs, dataset [eGeneralMedical] comprising of variety of murmur cases was used in the experiments. Figure 4.15 shows the obtained results of denoising using various methods for few cases of murmurs. From the figure, it can be observed that the proposed method suppressed the murmurs significantly in all cases. As expected, this improved the accuracy of the segmentation as shown in Table 4.3. However, in the case of aortic stenosis, mitral valve prolapse, pulmonary stenosis and tricuspid regurgitation, few components were undetected and hence false points are observed. This is because the murmurs significantly overlap the frequency range of the FHS. In these cases, the signal needs to be decomposed into narrow frequency bands.

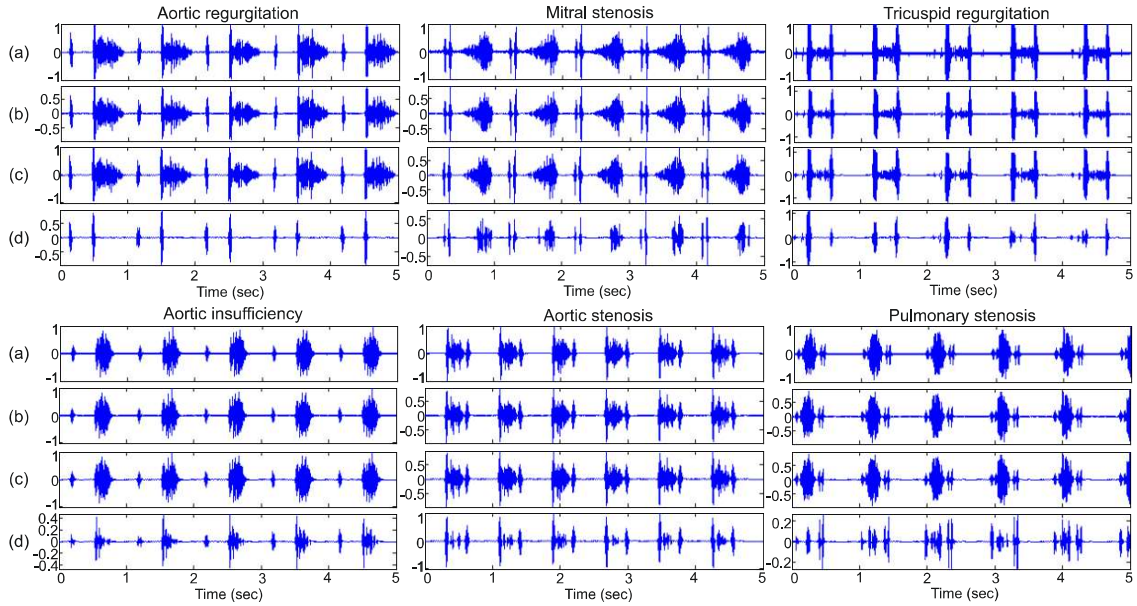

Figure 4.15 : Results of various methods to remove murmurs from the PCG signal; (a) murmur signal, (b) DWT- A method, (c) DWT-B method, and (d) Proposed method

Table 4.3 : Result for PCG signal with murmur

Murmur	Number of cases(cycles)	% of S1 detection			% of S2 detection			False points		
		DWT A	DWT B	Proposed	DWT A	DWT B	Proposed	DWT A	DWT-B	Proposed
Aortic stenosis	6(45)	100	100	100	88.8	88.8	100	28	28	4
Aortic insufficiency	1(6)	100	100	100	100	100	100	1	2	0
Mitral stenosis	1(8)	100	100	100	100	100	100	0	0	0
Aortic regurgitation	1(6)	100	100	100	100	100	100	4	4	0
Physiology split S2	1(4)	100	100	100	100	100	100	0	0	0
Pulmonary regurgitation	1(7)	100	100	100	100	100	100	7	7	0
tricuspid stenosis	1(4)	100	100	100	100	100	100	0	0	0
Wide split S2	3(15)	100	100	100	100	100	100	0	0	0
Ejection click	3(18)	100	100	100	100	100	100	0	0	0
Opening snap	1(6)	100	100	100	100	100	100	3	3	0
Mitral valve prolapse	5(29)	55.1	55.1	100	82.7	82.7	96.5	28	26	14
Mitral regurgitation	2(19)	100	100	100	89.4	89.4	100	4	4	0
Pulmonary stenosis	2(19)	68.4	68.4	84.2	100	100	100	6	6	5
Tricuspid regurgitation	2(14)	100	100	100	100	100	100	8	8	3

4.2 A METHOD FOR CANCELLATION OF MOTION ARTEFACTS FROM THE SEISMOCARDIOGRAM SIGNAL

As discussed above, the proposed DWT based denoising algorithm efficiently suppresses the level of noise from the heart sound signal. However, it leaves a lot of scope to improve the SNR particularly in case of walking scenario. These contaminations may corrupt the diagnostic features in the signal. Therefore, cancellation of these noise components is important to improve the usefulness of heart sound signal, while the subject is walking. The proposed method for motion artefact cancellation is discussed in the following subsections.

4.2.1 Introduction

Recently, an algorithm has been proposed to reduce the impact of motion noise from the SCG signal, based on averaging theory [Rienzo et al., 2013a]. In another method, an LMS based adaptive filter has been proposed to cancel the motion noise from the SCG signal [Yang and Tavassolian, 2015]. However, these algorithms require a reference signal or manual intervention to extract the cardiac cycles. In another approach, Pandia et al. [Pandia et al., 2010] implemented a polynomial smoothing filter to remove motion artefacts from the SCG signal generated due to walking. However, it only removes the low-frequency noise. DWT based denoising algorithms are able to suppress the in-band noise [Cai and Harrington, 1998]. However, it also will not be helpful in the walking scenario, as the intensity of the noise components is larger than the intensity of the heart signal components.

To address the issue of noise contamination in 'walking' scenario, a novel algorithm is presented to remove motion noise from the SCG signal. The z-axis and x-axis signals were recorded using a three-axis accelerometer, attached to the chest wall of the subject. The z-axis is set to perpendicular to the chest wall, and the x-axis is set in ventral-dorsal direction. Thus, heart signal components are presented prominently in the z-axis and the impact of walking is presented in the x-axis. Thus, to remove the noise components from the z-axis, locations of footsteps are identified from the x-axis. Then the corresponding noise from the z-axis signal is removed. After the removal of the noise components, the fundamental heart sound components, S1 and S2, are identified.

4.2.2 Impact of Noise on the x-axis and z-axis of the Accelerometer

The x-axis and z-axis signals were acquired in various real-life scenarios, including subject in motion while working in the office, speaking, and walking. A three-axis MEMS accelerometer (MMA-7361, Freescale Semiconductor) was attached to the chest wall, close to the apex of the heart. The acquired signals are fed to a PC through its sound card. The sound card significantly attenuates the signal below 10 Hz frequency, which is suitable for the

heart sound signal. The signals are then sampled at 2k frequency and stored in the PC. This sampling frequency is sufficient for the heart sound signal as their components, including fundamental and pathological, lie below 700 Hz [Debbal and Bereksi-Reguig, 2008a].

The acquired signals are filtered using a band-pass filter with 10-60 Hz band-pass frequency. This range of the filter is set because the frequency range of FHSs lie in this range [Jain et al., 2016]. The signals acquired in different scenarios are described in following subsections.

(a) Speaking

The SCG signals were recorded while the subject was speaking and plotted in the Figure 4.16. From the Figure 4.16(a), it can be observed that, due to speech of the subject, the acquired z-axis signal significantly affected. However, most of the contamination is out-of the frequency band of the FHS. It can be attenuated using a band-pass filter, as shown in the filtered signal (Figure 4.16(b)). There is negligible impact of the speaking of the subject on x-axis signal, as shown in Figure 4.16(c).

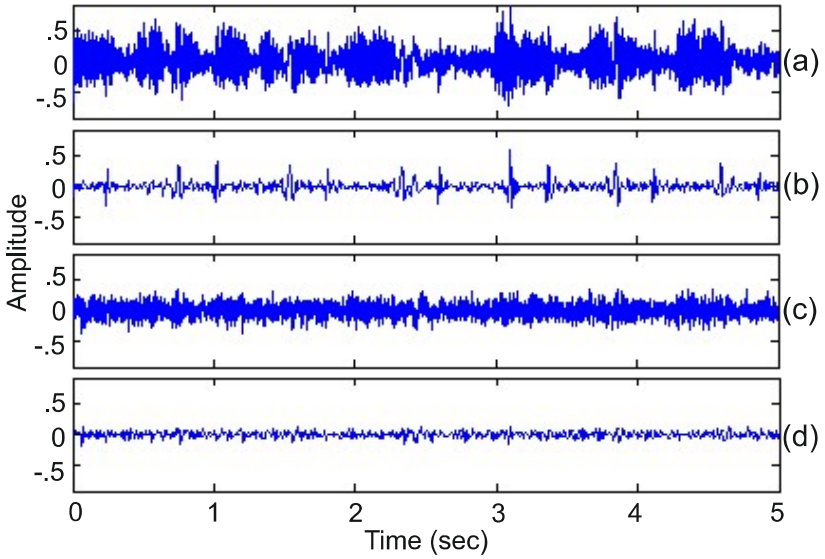

Figure 4.16 : Signals for speaking scenario: (a) Acquired z-axis signal, (b) Filtered z-axis signal, (c) Acquired x-axis signal, and (d) Filtered x-axis signal

(b) In Motion

The SCG signals were also recorded while the subject was in motion and working in the office. The recorded signals and their filtered versions are shown in the Figure 4.17. From the filtered z-axis signal, it can be observed that the heart signal is less affected due to slow motion noise. This is due to the better attachment of the accelerometer to the body, as discussed previously.

(c) Walking

The SCG signals were also acquired when the subject was walking and plotted in the Figure 4.18. In the z-axis signal, Figure 4.18(a), there are two types of noise contaminations. One is composed of low-frequency due to the motion and another is high-frequency components, which occur due to the footsteps. From the filtered z-axis signal (Figure 4.18(b)), it can be observed that the low frequency noise components can be attenuated by band-pass filtering. However, some noise components (marked as a red square) are presented due to footsteps, as shown in Figure 4.18(b). Figure 4.18 (c) and (d) show that the signature of the footsteps is also manifest in the x-axis signal.

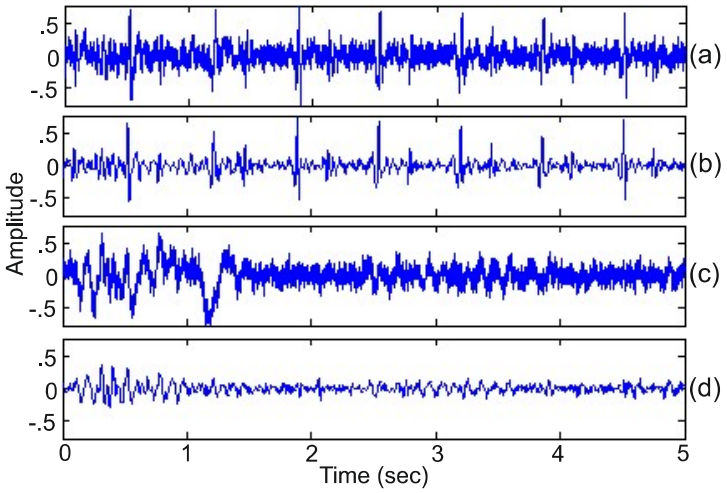

Figure 4.17 : Signals for motion scenario: (a) Acquired z-axis signal, (b) Filtered z-axis signal, (c) Acquired x-axis signal, and (d) Filtered x-axis signal

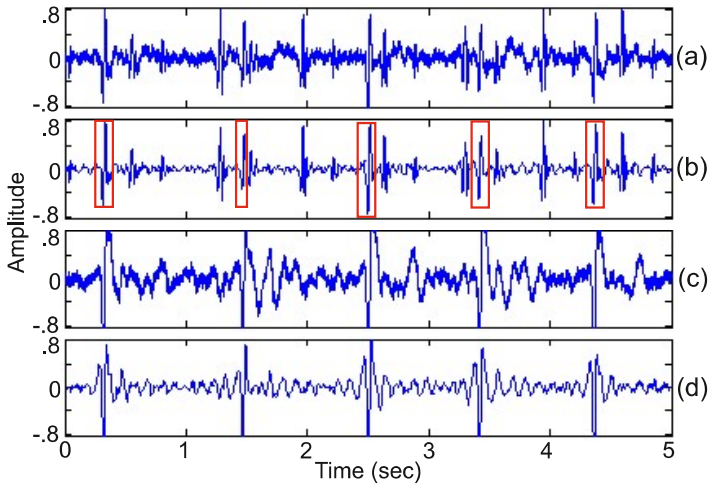

Figure 4.18 : Signals for walking scenario: (a) Acquired z-axis signal, (b) Filtered z-axis signal, (c) Acquired x-axis signal, and (d) Filtered x-axis signal

4.2.3 Methodology

The steps performed in the proposed algorithm are shown in the Figure 4.19. In the first step, the acquired signals of both axes (z-axis and x-axis) are filtered using a band pass filter with 10-60 Hz pass-band. Then, it is identified that footsteps are present or not, based on kurtosis of the x-axis. Kurtosis measures, whether the data is peaked or flat relative to the normal distribution [Pearson, 1905]. That is, data sets with low kurtosis tend to have a flat top near the mean rather than a sharp peak and vice-versa. Thus, the kurtosis value will be higher in case of footsteps are present, compared to the case when footsteps are not present. Therefore, if kurtosis is greater than threshold value T, footsteps are identified. Empirically, the value of threshold T equals to 10, found suitable.

If the footsteps are present, then their locations are identified in the x-axis signal using a threshold T_x. The value of threshold, T_x, is estimated using Otsu's method. Otsu's method estimates a threshold to classify a dataset into two classes such that the intraclass variance

will be minimum [Otsu, 1979].

The next step is to make the sample values zero in the z-axis signal, corresponding to the identified locations of footsteps in the x-axis signal. The extra (noise) component caused by the footstep in the z-axis signal may overlap the FHS, as shown in Figure 4.20. The corresponding location of the identified footstep in the z-axis signal is shown as a red point in this figure. If a window with fixed length is used to remove the noise components from the z-axis, it may also remove the heart sound components when they overlap, as shown in Figure 4.20(b) and (c). Therefore, we calculate zero-crossing points around the location of footsteps in the z-axis signal and then make values zero from two zero-crossing points before and after it.

After noise removal, peaks are detected in the filtered z-axis signal using a threshold value T_z, which is also estimated using Otsu's method. If two peaks are identified in 150 ms duration, then only one peak with higher amplitude is considered. This duration is selected to avoid multiple peaks for single component as the typical time duration of S1 and S2 remains 70-90 ms [Singh and Anand, 2007]. Then, the peaks are classified as S1 or S2 based on medical domain knowledge that the amplitude of S1 is higher than the amplitude of S2 and the duration between S1 to S2 is lower than the duration between S2 to S1 [Singh and Anand, 2007].

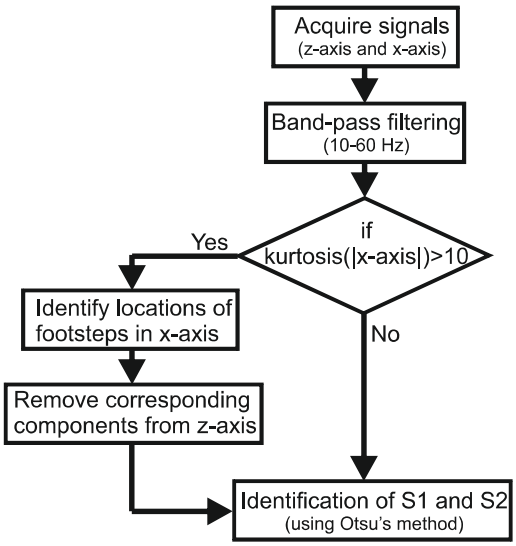

Figure 4.19 : Block diagram of the proposed method

4.2.4 Results and Discussion

The proposed method is applied to the acquired SCG signals in different noise scenarios. In speaking and motion scenarios footsteps will be absent, while, there will be footsteps in walking scenario.

The results of the proposed method are also compared with two state-of-art methods. One is based on DWT [Messer et al., 2001] and another based on Savitzky Golay based polynomial smoothing [Pandia et al., 2010]. In DWT based denoising algorithm, the signal is first decomposed up to five levels using 'coif5' as a mother wavelet. Then 'rigrsure' threshold estimation method with soft threshold function is used to suppress the noisy coefficients. For the peak detection, same method as in the proposed method is used. The obtained results for both cases are described as follows.

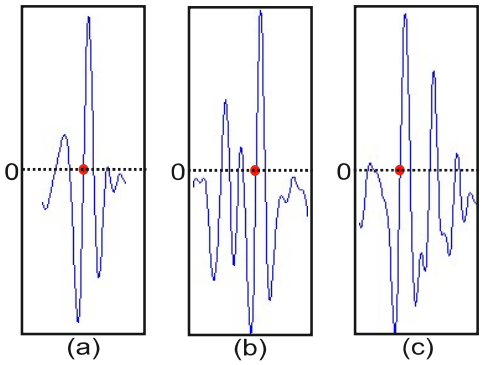

Figure 4.20 : Noise components in z-axis due to footsteps: (a) Noise component, (b) Noise component after the heart sound component, and (c) Noise component before the heart sound component

Case 1: Without Footsteps (Speaking / Motion)

The obtained results of the proposed method and compared methods are shown in Figure 4.21, for the signal recorded in motion scenario. When there are no footsteps, the kurtosis value of the x-axis will be low and thus it is identified that the signal is without footsteps. The identified peaks in the filtered z-axis using the DWT, polynomial smoothing filtering, and the proposed method are shown in Figure 4.21(c), (d), and (e), respectively. From the figure, it can be observed that all three methods are able to suppress the noise from the signal, and hence S1 and S2 are detected efficiently.

Case 2: With Footsteps

The obtained results of the proposed method and compared methods for walking scenario are shown in Figure 4.22. The identified peaks in the filtered z-axis signal using the proposed method and compared methods are shown in Figure 4.22(c-e). According to the proposed method, first, the locations of footsteps are identified in the x-axis signal. Then, the noise components corresponding to the footsteps are removed from the z-axis signal, as shown in Figure 4.22(e). From the figure, it can be observed that the proposed method efficiently identified and remove the noise components (footsteps) from the z-axis and accurately identified heart sound components. Both the compared methods suppressed the low-frequency noise significantly. However, both methods could not remove the noise components generated due to footsteps and results into noise peaks remained in the filtered signal.

The proposed method and the compared methods are applied to the acquired signals from a number of subjects in various scenarios. The obtained results are given in Table 4.4. From the table, it can be observed that the proposed method efficiently works in each scenario and outperforms the competitive methods. However, there were few false peeks remained in the filtered signal using the proposed method. It is due to the number of noise components generated by a single footstep.

4.3 CONCLUSIONS

In this chapter, we have proposed a DWT based method for denoising of the heart sound signal. The main contribution of the work is to threshold the wavelet coefficients adaptively, according to the presence of noise. For the estimation of the threshold value, the method uses the domain knowledge about the heart sound signal that the sum of the length of the S1 and S2 remains less than 25% of the length of a cardiac cycle. We also proposed a non-linear

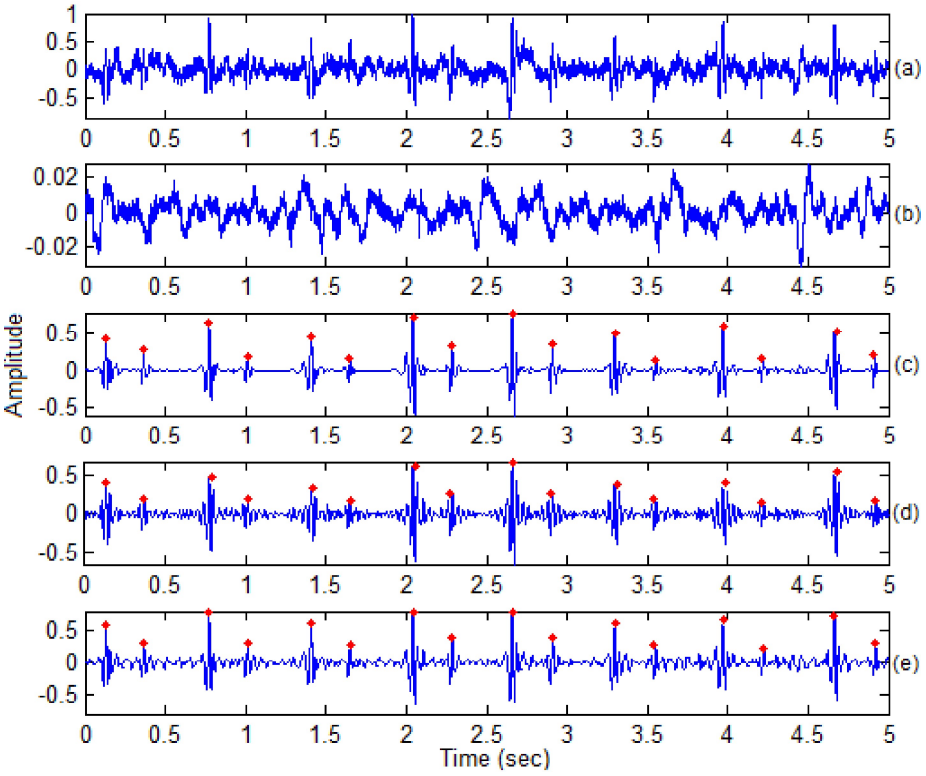

Figure 4.21 : Obtained results for 'in motion' scenario: (a) Acquired z-axis signal, (b) Acquired x-axis signal, and (c-e) Identified peaks in the filtered z-axis signal using DWT (c), polynomial smoothing filtering (d), and (e) the proposed method

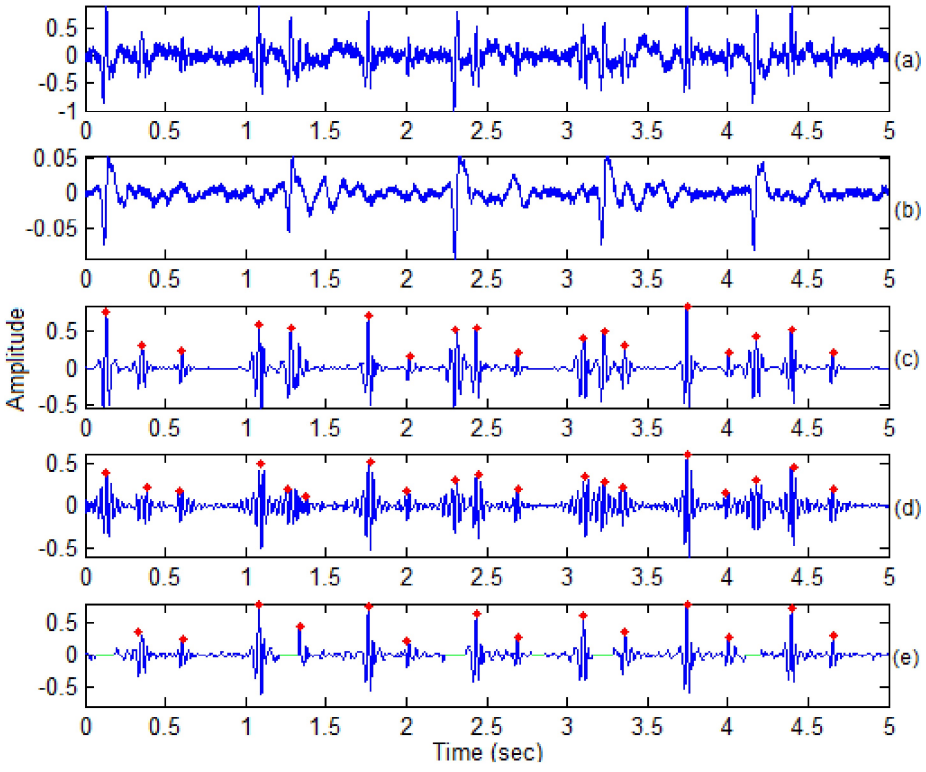

Figure 4.22 : Obtained results for 'walking' scenario: (a) Acquired z-axis signal, (b) Acquired x-axis signal, and (c-e) Identified peaks in the filtered z-axis signal using DWT (c), polynomial smoothing filtering (d), and (e) the proposed method

Table 4.4 : Obtained detection rate of S1 and S2, and number of false points in various scenarios

	Footsteps	S1 detection rate (%)			S2 detection rate (%)			Number of false points		
		DWT	polynomial	proposed	DWT	polynomial	proposed	DWT	polynomial	proposed
Speaking										
Subject 1	0	100	100	100	92.3	96.1	100	2	1	0
Subject 2	0	100	100	100	96.1	96.1	100	1	2	1
Subject 3	0	100	100	100	100	100	100	0	0	0
Subject 4	0	100	100	100	88.4	92.3	100	1	2	0
Subject 5	0	100	100	100	93.1	96.5	96.5	3	2	1
Motion										
Subject 1	0	100	100	100	93.3	90.0	93.3	2	4	1
Subject 2	0	100	100	100	100	100	100	1	1	1
Subject 3	0	100	100	100	95.8	95.8	100	1	1	0
Subject 4	0	95.8	95.8	95.8	91.6	91.6	91.6	4	4	2
Subject 5	0	100	100	100	100	100	100	0	0	0
Walking										
Subject 1	12	100	100	100	79.3	75.8	93.1	13	14	3
Subject 2	16	96.5	100	100	86.2	86.2	93.1	12	15	2
Subject 3	14	92.6	92.6	96.3	92.8	96.4	100	13	13	3
Subject 4	17	96.0	92.0	96.0	92.0	80.0	96.4	16	18	2
Subject 5	23	96.1	96.1	96.1	73.0	80.7	100	22	20	5

mid threshold function and optimised its parameter for the PCG signal. The performance of the method is analysed for various types of simulated noise including white Gaussian noise, pink noise, and red noise. Performance is also compared for the signals recorded in various real-life scenarios. The obtained results show that the proposed method outperforms the state-of-the-art methods. However, it is observed that additional algorithm is required to remove in-band noise signature due to footsteps when the subject is walking. In walking scenario, it is observed that the undesired footstep signature of noise component has larger amplitude compared to the FHS. To address this issue, a novel motion noise cancellation method using the multiple axes of an accelerometer has been presented. The obtained results show the effectiveness of the proposed method to remove the noise components generated due to footsteps.

In the motion noise cancellation method, if footsteps are detected in the x-axis signal then it removes the corresponding components from the heart sound signal (z-axis), and if footsteps are not detected in the x-axis signal, it does not process the z-axis signal. Therefore, we propose to use the motion noise cancellation method in combination with the DWT based denoising algorithm to suppress the in-band noise as well as noise generated due to footsteps. Such method makes a system able to perform heart monitoring in real-life scenarios.

In addition to noise generated due to external sources, the noise removal method should also be able to suppress the murmur from the FHS. Murmurs are the pathological sound, which may overlap the FHS in time and frequency domain, both. Murmur should be separated from the FHS to segment the heart sound signal into separate cardiac cycles. Segmentation of the signal is important because the diagnostic features can be extracted more accurately from the segmented cardiac cycles as compared to the signal without segmentation. Therefore, the proposed DWT based method is also tested to suppress the murmur from the FHS. The obtained results show that the method is able to emphasise the S1 and S2 in the presence of murmurs as well. However, in few cases of murmurs when the murmur overlaps the FHS significantly, the proposed method needs improvisation. Therefore, the future work includes the decomposition of the signal into fine-tuned narrow frequency bands.

...